J Mater Sci (2009) 44:3867–3876
DOI 10.1007/s10853-009-3525-5

Compressive properties of a new metal–polymer hybrid material

Daniel R. A. Cluff · Shahrzad Esmaeili

Received: 1 December 2008 / Accepted: 27 April 2009 / Published online: 19 May 2009
© Springer Science+Business Media, LLC 2009

Abstract Compressive properties of a new hybrid material, fabricated through filling of an aluminum foam with a thermoplastic polymer, are investigated. Static (0.01 s^{-1}) and dynamic (100 s^{-1}) compression testing has been carried out to study the behavior of the hybrid material in comparison with its parent foam and polymer materials. Considering the behavior of metal foams, the point on a compressive stress–strain curve corresponding to the minimum cushion factor is defined as the "densification" point. The analysis of the stress–strain curves provides insight into the load carrying and energy absorption characteristics of the hybrid material. At both strain rates, the hybrid is found to carry higher stresses and absorb more energy at "densification" than the foam or polymer.

Introduction

There are many gaps remaining in material properties despite the extensive list of materials available. The presence of these gaps is especially true when a combination of properties is required [1]. Although some of the gaps can be filled by producing new alloys and polymers, the design of new material combinations can provide solutions to many engineering problems. Hybrid materials, an amalgamation of two or more monolithic materials combined in a predetermined shape and scale, display properties which are combinations of those displayed by the parent materials [2]. The term hybrid material encompasses both traditional composite materials, such as carbon fiber-reinforced polymers, and shape-based material combinations, such as sandwich panels (i.e., solid face sheets separated by a foam core) [1].

Metallic foam, a hybrid material in its own right (i.e., metal–air), has elicited growing interest over the past 25 years. This is demonstrated by the numerous investigations into metallic foam processing, characterization, and properties [3–17]. Aluminum foams are among the most prominent metallic foams due to their desirable processability and mechanical properties. A high specific strength, stiffness, and energy absorption [9, 14, 18–20] lead to many potential applications for aluminum foam and aluminum foam-based interconnected composites in various transportation industries (e.g., automotive, aerospace, rail) [10, 17, 21]. Although fabricated in an open- or a closed-cell configuration [10], an open-cell foam leaves open the possibility of filling with a second material. Polymers are also considered to be lightweight and can display good energy absorption properties [21].

Research has shown that if a viscous fluid were introduced into an open-cell foam, an increase in energy associated with the flow of the fluid would be required to compress the hybrid structure [5, 21, 22]. Thermosetting polymers have been utilized to fill open-cell aluminum foams [11, 21–23]. In the work by Cheng and co-workers [21, 22], the filled foam has shown better energy absorption capacity and efficiency compared to the base aluminum foam [21, 22]. Kwon et al. [11] has studied the effective elastic moduli and failure strengths of polymer-filled aluminum foams using the finite element method on a tetrakaidecahedral unit cell. They have also used experimental work to validate their model [11]. More recently, Jhaver and Tippur [23] have utilized AA6101 Duocel® open-cell

D. R. A. Cluff · S. Esmaeili (✉)
Department of Mechanical and Mechatronics Engineering, University of Waterloo, 200 University Ave. West, Waterloo, ON N2L 3G1, Canada
e-mail: shahrzad@uwaterloo.ca

aluminum foam to enhance the compressive strength and energy absorption properties of an epoxy-based syntactic foam. Stöbener et al. [24] have developed an alternate method of producing an aluminum foam–polymer hybrid using closed-cell aluminum foam elements of varying size (5–15 mm) joined by a polymeric adhesive. Their research has shown that below a global strain of 30%, the polymer joint is the weak link. Above 30% strain, the hybrid behaves similar to a typical closed-cell aluminum foam, and the energy absorption of the hybrid is shown to be competitive with commercial aluminum foams. Wang et al. [25] have reported fabrication of a titanium/polymer biocomposite, using commercially pure Ti to produce porous Ti and high-density polyethylene or polyurethane for filling of the foam.

This work is based on a new design concept which included filling open-cell metallic foams with thermoplastic polymers to ensure full recyclability of the new hybrid materials for applications such as energy absorbing parts in transportation. Based on this concept, a new prototype material has been developed using AA6101 Duocel® open-cell aluminum foam and an ethylene vinyl acetate co-polymer of trade name Elvax®. This article reports a study on the mechanical response of this newly developed hybrid material in comparison with its parent materials' behavior under the same conditions of static or dynamic compressive loading.

Experimental methods

Material and fabrication method

AA6101 Duocel® open-cell aluminum foam with a nominal relative density of 6–8% and a pore size of 10 pores per inch (ppi), corresponding to 0.4 pores per millimeter, is used in this investigation. Foam blocks, with the dimensions 51 × 254 × 254 mm^3, were obtained from ERG Materials and Aerospace Corporation, Oakland, CA in as-fabricated condition with no further heat treatment performed. The polymer utilized to fill the aluminum foam is an ethylene vinyl acetate co-polymer of trade name Elvax® 205 W. Elvax® 205 W has an MI of 800 [26] and a melting temperature of 74 °C [27]. The polymer was provided by DuPont in the form of pellets with an approximate diameter of 3 mm.

The aluminum foam test samples are cut into rectangular-based blocks of 38 × 38 × 51 mm^3 on a band saw with the long dimension in the direction of cell elongation. These dimensions ensure at least eight cells in each direction, eliminating sample size effects [9]. The hybrid specimens utilize an aluminum foam specimen as the interconnected component. The aluminum foam specimen is placed in an aluminum mold and then filled with molten Elvax® to produce the hybrid material specimen. The specimen fabrication procedure has been described in [28]. It should be noted that the top and bottom faces of the hybrid specimens are machined with an end mill to ensure that the aluminum foam structure is in direct contact with the platens during compression testing and that the surfaces are parallel. Nominal hybrid specimen dimensions are 39 × 39 × 50 mm^3. A picture of a hybrid specimen is shown in Fig. 1.

The polymer test specimens are created by filling the same aluminum mold utilized to fabricate the hybrid specimens with molten polymer. The solidified polymer is then cut to final dimensions on a band saw, and the top and bottom faces are milled to ensure coplanarity. The polymer specimens are smaller due to shrinkage and have a nominal size of 36 × 36 × 44 mm^3. Although the three materials have slightly different dimensions, the height-to-thickness ratios are equivalent in all three cases.

Testing

Compression testing is performed in the direction of cell elongation. Prior to compression testing, sample dimensions are measured with digital calipers to an accuracy of 0.1 mm. The recorded force–displacement data is converted to engineering stress and strain values based on the measured sample dimensions. A minimum of two tests are performed for each material under each testing condition.

Static testing is performed on a screw-driven Instron 4208 at a crosshead speed of 25 mm/min. This corresponds to a strain rate of approximately 0.01 s^{-1} for all three

Fig. 1 The as-fabricated aluminum foam–polymer hybrid specimen

materials. Testing is automatically halted when the preset load limit of 70 kN is reached. This load level ensures full compression and hence force–displacement data beyond foam densification.

Dynamic testing is conducted on an Instrumented Falling Weight Impactor (IFWI) Type 5 HV fitted with an Imatek controller. An enhanced laser velocity system measures the displacement of the anvil. Force is measured with a KISTLER ± 100 kN piezoelectric load cell. Reference [29] gives a detailed account of the IFWI. A strain rate of 100 s^{-1} is chosen for dynamic testing. To achieve this strain rate, the necessary impact velocity (v_{imp}), impact mass (m_{imp}), and drop height (h_{drop}) are calculated using the initial height of the specimen (h_o), the desired strain rate ($\dot{e}$), and an estimate for total amount of energy absorbed by the specimen (E) as follows:

1. The equation for strain rate is rearranged to solve for velocity $\rightarrow v_{imp} = \dot{e} \cdot h_o$.
2. The equation for kinetic energy of impact is equated with that of the potential energy before the release of the anvil to solve for drop height $\rightarrow h_{drop} = v_{imp}^2/(2 \cdot g)$, where g is the acceleration due to gravity.
3. Finally, the impact mass is calculated by the equation for potential energy $\rightarrow m_{imp} = E/(g \cdot h_{imp})$, where E is taken as the total amount of energy absorbed in joules during static compression testing.

Table 1 indicates the parameters utilized for performing dynamic testing. For this analysis, only data collected prior to the anvil reaching a downward velocity of 0 m/s is utilized. It is noted that the strain rate of 100 s^{-1} is only the initial strain rate. The rate changes as the impactor slows and the specimen becomes shorter. Dynamic testing on the drop tower produces initial vibrations caused by impact which are visible in the results (i.e., false curve fluctuations) [29, 30]. To avoid filtering out real data, the results are left as-is without filtering.

Nomenclature

The following describes the parameters that are used to report the analysis of the test data.

Table 1 Impactor mass, height, and speed utilized for drop testing

Material	Impactor		
	Mass (kg)	Height (m)	Speed (m/s)
Aluminum foam	13	1.3	5.1
Polymer	13	1.0	4.4
Hybrid	23	1.3	5.1

- *Specific energy absorbed* (W) is the area under the stress–strain curve normalized with the sample volume. The total specific energy absorbed is taken as the normalized area under the stress–strain curve at e_d.
- *Cushion factor* (C) is a measure of energy absorption efficiency defined by the peak stress divided by the specific energy absorbed, $C = \sigma/W$ [5]. For each set of the stress–strain data points, the highest recorded stress from 0 strain up to e is divided by W up to the strain e. The cushion factor is also used in this investigation to discuss energy absorption efficiency, where a lower cushion factor indicates higher energy absorption efficiency.
- *Stress plateau* is the name given to the section of the stress–strain curve where the stress remains almost constant despite increasing strain. It is well described in [5].
- The point of "*densification*" is defined as the strain where the cushion factor (C) is a minimum. This approach is similar to that taken by Fuganti et al. [31] who utilize force–displacement instead of stress–strain and term the value "total efficiency". Figure 2 shows a typical foam stress–strain curve plotted with the cushion factor indicating both the densification stress (σ_d) and the densification strain (e_d). It should be noted that the term "densification" is used loosely as both the hybrid and the polymer are solid and hence are dense prior to compression. This term, typically utilized in foams for the end point of the stress plateau, is maintained for the hybrid and the polymer for consistency in dealing with the common observable phenomena for the point of highest energy absorption efficiency.

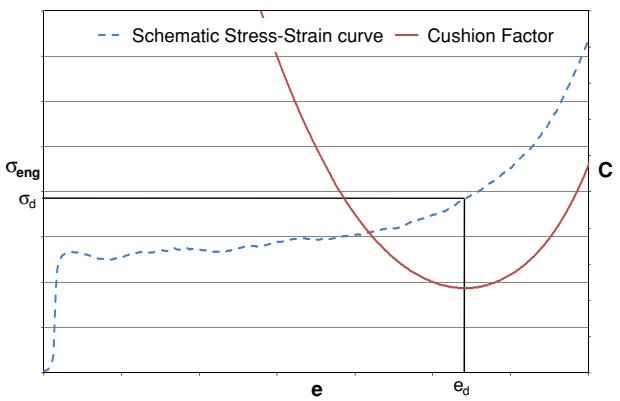

Fig. 2 Schematic presentation of a typical engineering stress (σ_{eng})–strain (e) curve for a foam specimen, demonstrating how the point of densification is determined using the cushion factor

Results and discussion

Static compression testing

Figure 3 shows the typical appearance of the specimens post static compression testing. During static compression testing, the aluminum foam is seen to compress in multiple deformations bands [28]. These discrete crush bands have also been observed by other researchers [13]. Little lateral deformation is observed with the dominant deformation mechanisms being cell wall buckling and bending [5]. The polymer, however, displays significant lateral deformation during loading and displays some strain recovery upon unloading. This lateral expansion of polymer specimens indicates that the polymer used in this study attempts to maintain its original volume under uniaxial compression. Similar to the polymer, the hybrid specimen deforms laterally during loading and displays strain recovery when the load is removed. As the polymer obscures the foam ligaments inside the hybrid, the effect of the lateral deformation on the ligaments cannot be examined during testing. However, by removing the polymer post compression testing, it is revealed that some ligaments have deformed by bending or buckling while some segments have completely fractured. This can be seen in Fig. 3d) where a discontinuous ligament network is evidenced when the polymer is removed by heating. Unlike the foam, which has empty cells accommodating the deforming aluminum, the hybrid is a solid specimen comprised mostly of the polymer (~93 vol.%). The lateral expansion of the aluminum foam–polymer hybrid material can therefore be attributed to the stress–strain behavior of the polymer used in filling the foam. This observation is similar to that observed by Cheng and Han [21] during the compression of aluminum foam filled with silicone. Cheng and Han attribute the lateral expansion of their polymer-filled foam to the incompressibility (i.e., maintenance of constant volume during deformation) of the silicone. The lateral expansion of the polymer is also the cause of the fractured ligaments. The ligaments prevent the polymer from expanding; however, when the compressive stress is large enough (producing large forces normal to the loading direction on the ligaments by the expanding polymer), the ligaments fail allowing the polymer to flow out [21, 22].

Typical stress–strain curves for the test specimens can be seen in Fig. 4. The curves obtained for the aluminum foam specimen is what would be expected for a typical elastic–plastic metallic foam with a well-defined stress plateau prior to densification [5]. The foam shows an approximate densification strain of $e_d = 0.6$. The polymer, on the other hand, displays a typical stress–strain trend in elastomeric materials [32], with a low, near constant, stress–strain slope up to a strain of approximately $e = 0.5$, whereupon the slope rapidly increases. Co-incidentally, the polymer's point of densification also occurs at an approximate strain of $e_d = 0.6$.

There are both similarities and differences between the stress–strain curves of the hybrid material and the parent materials. To demonstrate these similar and different features, the stress–stress curve of the hybrid material is

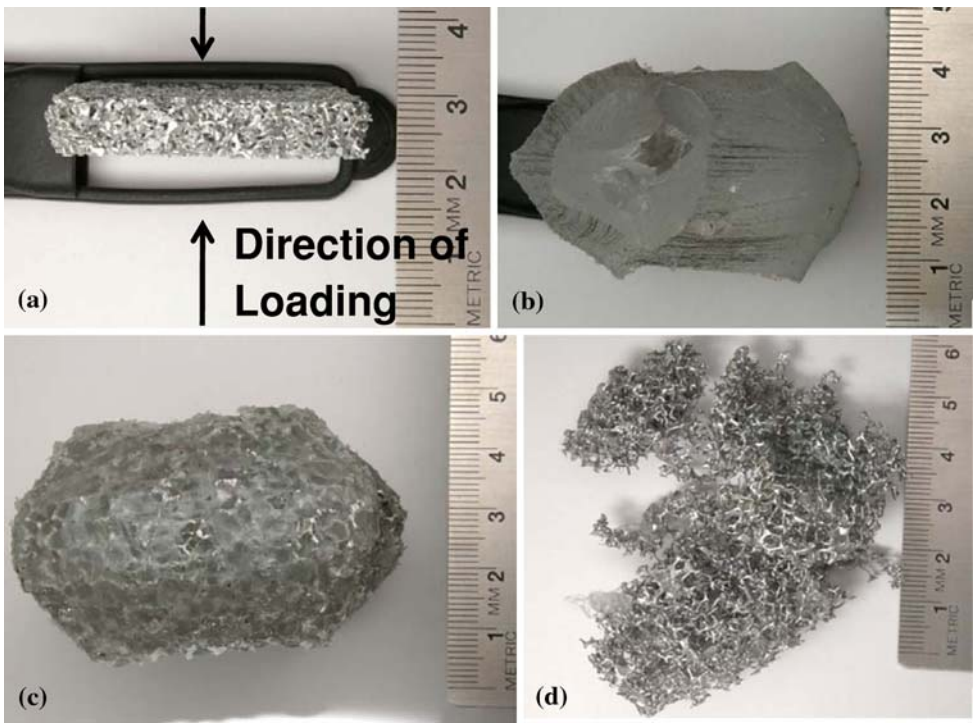

Fig. 3 Typical specimen appearance post static compression. **a** Aluminum foam. **b** Polymer. **c** Aluminum foam–polymer hybrid. **d** Aluminum foam–polymer hybrid specimen after the removal of the polymer

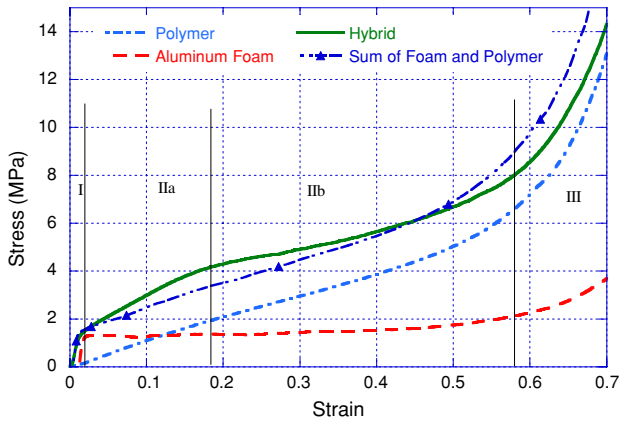

Fig. 4 Compressive stress–strain curves for the polymer, aluminum foam, and aluminum foam–polymer hybrid under static compression. The linear sum of the curves for the polymer and foam is also shown

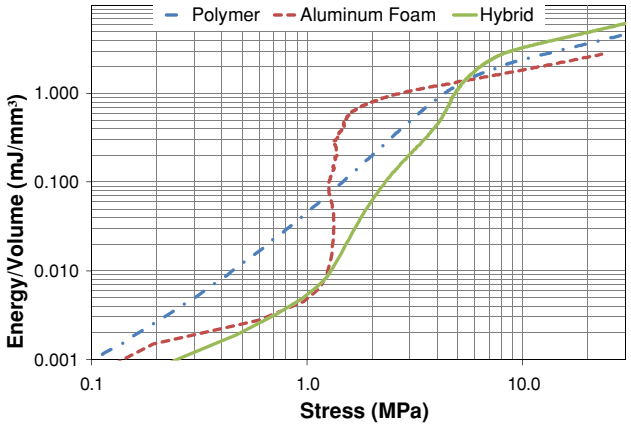

Fig. 5 Energy absorption curves for the polymer, aluminum foam, and aluminum foam–polymer hybrid under static compression

divided into different regions, as shown in Fig. 4. In Region I, which is below a strain of approximately 0.03, the stress–strain curves of the hybrid and the aluminum foam are similar. This is expected since the polymer displays low stiffness and low stress values compared to the foam at this stage, and thus is not expected to carry much load. On the other hand, in Region III, which starts from an approximate strain close to the densification strain of all three materials, the stress–strain curves of the hybrid and the polymer become similarly steep.

In between Regions I and III, the stress–strain curve of the hybrid material has features that appear to reflect an interaction between the parent materials. To better see the interaction effect, Fig. 4 also plots the linear sum of the parent materials' stress–strain curves (i.e., $\sigma_{\text{sum}}(e) = \sigma_{\text{polymer}}(e) + \sigma_{\text{foam}}(e)$). It appears that in Region IIa, as in the case of the polymer, the trend of change in stress with strain is linear for the hybrid material. The stress–strain slope for the hybrid is, however, steeper than the slope of the curve for the polymer or the summation curve shown in Fig. 5. Region IIb is characterized by a decrease in the slope of the hybrid material's stress–strain curve, with the hybrid material's behavior gradually approaching that of the polymer.

The shape of the stress–strain curve for the foam suggests that plastic deformation in the foam structure occurs in Region II [5, 8]. The increase in strength of the hybrid material can be related to the interactions between the plastically deformed foam ligaments and the elastoplastic deformation of the polymer, particularly the resistance to polymer expansion imposed by the aluminum foam ligaments. In the previous works on aluminum foam filled with thermosetting polymers, both Cheng and Han [21], and Kwon et al. [11] attributed the increase in strength to the support provided by the polymer against ligament bending and buckling. Cheng and Han [21] also noted that some of the increase in strength could be due to the effect the ligaments had on the polymer. More specifically, these researchers attributed the increase in strength to the prevention of polymer expansion by the ligaments due to the creation of a tri-axial state of compressive stress in the polymer and the resultant increase in the apparent stiffness of the polymer [33]. It is likely that the mechanism explained by Cheng and Han [21] is responsible for the increase in strength, beyond a linear addition of the stress contributions from the foam and the polymer, in the current hybrid system. With the lack of verified mechanisms and consistent with the observed behavior, it is hypothesized that gradual fracture of aluminum foam ligaments in Region IIb produces a decrease in the slope of the hybrid material's stress–strain curve. In particular, the behavior is associated with two combined factors which lead to the observed decrease in slope. First, a disconnected cell structure decreases the resistance to polymer lateral expansion, decreasing the apparent stiffness of the polymer, and hence the measured stress, in the hybrid. Second, as the foam becomes disconnected, fewer ligaments contribute to the load carrying capacity of the foam in the hybrid. At the end of Region IIb, the stress–strain response approaches that of the polymer. This indicates most of the load is carried by the polymer and not the foam. Also reduction in interconnectivity of the aluminum foam network decreases the resistance to the recovery of strain in the polymer upon removal of load. This explains the difference between the measured strain upon testing and the observed final strain after unloading.

Considering Region III, the hybrid material appears to have a densification behavior similar to that of the polymer. This response further supports the interpretation of the results for the deformation behavior in Region IIb. In other words, as deformation progresses, the contribution of the foam to the load carrying capacity of the hybrid diminishes

until no further load is carried by the foam in Region III and the hybrid and the polymer approach almost the same densification response. This indicates that the foam ligaments within the hybrid are no longer continuous in the densification region. However to confirm the assertions about hybrid deformation mechanisms further investigation is required. It should be noted that the choice of the densification strain in this work is different from the report on the silicone rubber-filled aluminum foam [21] and therefore no direct comparison between the densification behavior in the two materials is made. However, the comparison of the shapes of the stress–strain curves for the two hybrid materials suggests that they behave differently under compression. The difference in the behavior of the two materials may not only be due to the use of different polymers in the two studies but also partly from the difference in the relative density of the aluminum foam used in the two studies.

Table 2 displays the properties of all three materials at the point of densification. In spite of similar densification strains for all three materials, the hybrid material displays the highest densification stress (7.2 MPa) and absorbs the highest specific energy up to densification (2.5 mJ/mm^3). To compare the energy absorption properties of the three materials, the amount of specific energy absorbed vs. stress is plotted in Fig. 5. For stresses below 2 MPa, the aluminum foam specimen shows a significant increase in specific energy absorption for a small increase in stress ($\sim$0.8 mJ/mm^3 from 1 to 2 MPa). However, beyond 2 MPa, the increase in W with increasing σ becomes smaller. Neither the polymer nor the hybrid material displays such an increase over such a small range. The polymer displays the highest specific energy absorption up to a stress of $\sim$1.2 MPa. Between 1.2 and 5 MPa, the aluminum foam absorbs the most energy. Beyond 5 MPa, the hybrid absorbs the most energy for a given stress.

Although the hybrid material absorbs more energy at densification, it has a higher cushion factor, and hence a lower energy absorption efficiency, when compared to the parent aluminum foam. In fact, considering cushion factors, aluminum foam is the most efficient energy absorber of the three materials with the lowest value of $C = 2.5$. The hybrid material shows improvement in both the total energy absorbed and the energy absorption efficiency at densification compared to the polymer. Although a multitude of the selection criteria should be considered in choosing a new material for any energy absorption application, the above simple analysis based on the cushion factor can provide a basis for the selection of the polymers for foam filling. This work suggests that a polymer with much lower stiffness could provide a lower stress but a higher densification strain for the hybrid and a higher energy absorption efficiency than the level achieved in this prototype material. The total amount of energy to be absorbed, maximum allowable force, contact area, and volumetric constraints [5] are among other important factors in choosing the parent materials for hybrid system fabrication and the resultant hybrids. These considerations require future detailed constitutive modeling and are beyond the scope of this work.

Table 2 Comparison of properties under static loading for aluminum foam, polymer, and aluminum foam–polymer hybrid

Material	e_d	Properties at e_d		
		σ_d (MPa)	W_d (mJ/mm^3)	C_d
Aluminum foam	0.6	2.0	0.8	2.5
Polymer	0.6	6.5	1.7	3.8
Hybrid	0.6	7.2	2.5	2.9

Dynamic compression testing

For this testing, visual observations during the impact are not made due to the high strain rate. However, the impacted specimens give insight into the deformation behavior during testing. Figure 6 depicts the specimens after the impact test. As shown, the shape of the affected aluminum foam is same as the shape of a specimen after static compression testing. In contrast, unlike during static compression testing where the hybrid and the polymer specimens had similar appearances after testing, the polymer displays near full recovery of strain, whereas the hybrid demonstrates permanent deformation characterized by a loss in height (i.e., 20%, approximately) and barreling. Although the level of barreling is not as extensive as in the statically tested specimen, the observation of full lateral expansion and the strain recovery in the hybrid is similarly attributed to the plastic deformation of the aluminum foam component and the tendency for full strain recovery in the polymer filling. Moreover, the observations of the full strain recovery in the polymer specimen, and not in the hybrid, indicate that the permanent deformation in the hybrid is due to the foam skeleton which is still effective albeit the broken struts as seen in Fig. 6d).

The typical stress–strain behavior of each material under dynamic loading (i.e., 100 s^{-1}) is shown in Fig. 7. As observed in all three curves, the curves are not smooth as under static loading. These fluctuations, which are similar to observations by Lifshitz et al. [34] and Shin et al. [35], are attributed to ringing in the impactor with the different materials attenuating the noise differently. The stress–strain curves obtained from the dynamic and static tests are compared in Figs. 8, 9, and 10. Examination of the stress–strain curves shows that the linear-elastic region of the aluminum foam, as clearly observed with the static

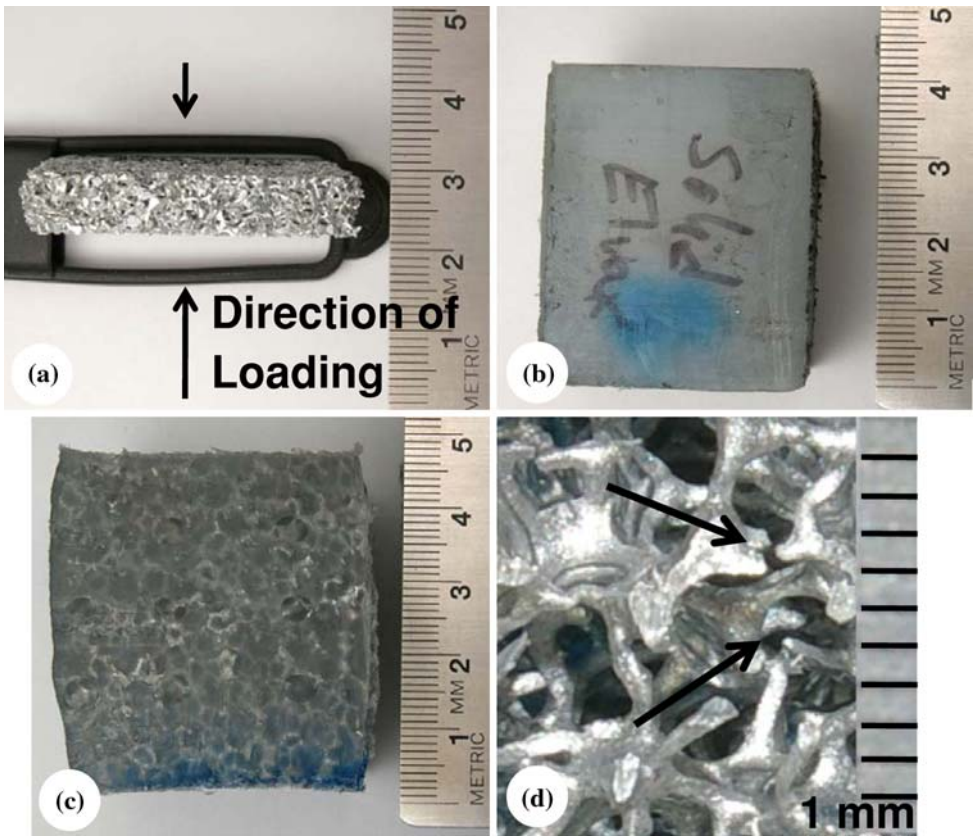

Fig. 6 Typical physical specimen appearance post dynamic compression. **a** Aluminum foam. **b** Polymer. **c** Aluminum foam–polymer hybrid. **d** Aluminum foam–polymer hybrid specimen after the removal of the polymer

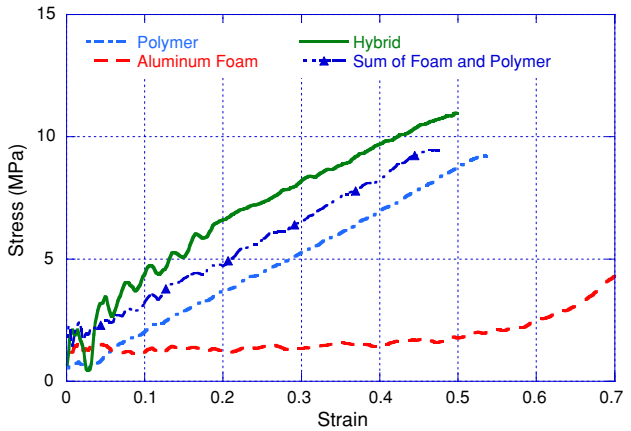

Fig. 7 Compressive stress–strain curves for the polymer, aluminum foam, and aluminum foam–polymer hybrid under dynamic compression. The linear sum of the curves for the polymer and foam is also shown

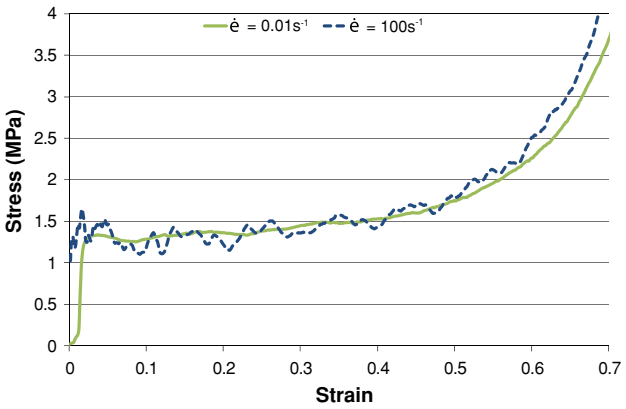

Fig. 8 Comparison of compressive stress–strain curves of aluminum foam under static (0.01 s^{-1}) and dynamic (100 s^{-1}) strain rates

compression testing, is not detectable in the dynamic test result. This can be attributed to the limitations associated with signal measurement in the current test. It should be noted that Deshpande and Fleck [7], Dannemann and Lankford Jr. [6], and McArthur et al. [12] all show a linear-elastic region in aluminum foams tested at very high strain rates using a Compressive Split Hopkinson Bar. Similar to the static test results, the stress–strain curve of the aluminum foam has a plateau where stress remains approximately constant up to the densification region. The dynamic compression test result for the polymer specimen also shows similarity with the static test result, displaying an approximately linear stress–strain curve up to the final, i.e. the highest achieved, strain in dynamic testing (i.e., $e_f \sim 0.5$). However, no subsequent sharp increase in stress with strain, as observed in static testing, i.e., no "densification," is observed for the polymer during the current dynamic testing (see Fig. 9).

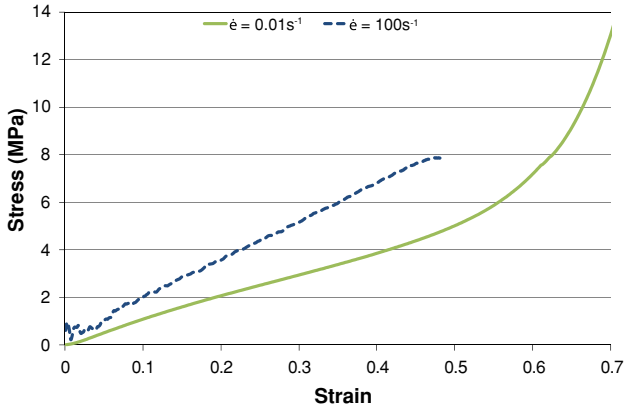

Fig. 9 Comparison of compressive stress–strain curves of the polymer under static (0.01 s^{-1}) and dynamic (100 s^{-1}) strain rates

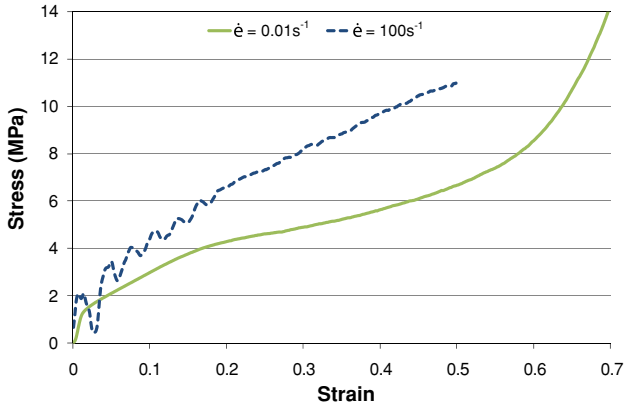

Fig. 10 Comparison of compressive stress–strain curves of aluminum foam–polymer hybrid under static (0.01 s^{-1}) and dynamic (100 s^{-1}) strain rates

The stress–strain curve of the hybrid material, as shown in Fig. 10, displays an overall shape similar to that of the polymer specimen, with a linear stress–strain trend in the entire measured limit of stress (ignoring the initial false fluctuations). Generally, considering either peaks or valleys of the fluctuations, the slope of the stress strain curve of the hybrid is larger than that of the polymer up to a strain of 0.20. Beyond $e = 0.20$, however, the slope of the stress–strain curve for the hybrid material reduces to the level displayed by the stress–strain curve of the polymer. Similar to the behavior of the polymer specimen, there is no "densification" point on the stress–strain curve of the hybrid material. This well explains the tendency for strain recovery in the hybrid material and supports assumptions of the maintenance of a semiconnected network of struts in aluminum foam component of the hybrid. The behavior of not achieving "densification" during testing is not only strain rate dependent, as shown in Fig. 10, but it is also a consequence of the low level of impact energy chosen in this work.

Table 3 Comparison of properties under dynamic loading for aluminum foam, polymer, and aluminum foam–polymer hybrid

Material	e	Properties at e_d or e_f		
		σ (MPa)	W (mJ/mm^3)	C
Aluminum foam	$e_d = 0.6$	$\sigma_d = 2.2$	$W_d = 0.9$	$C_d = 2.4$
Polymer	$e_f = 0.5$	$\sigma_f = 8.1$	$W_f = 2.1$	$C_f = 3.9$
Hybrid	$e_f = 0.5$	$\sigma_f = 10.4$	$W_f = 3.1$	$C_f = 3.4$

The properties of all three materials during dynamic compression testing are listed in Table 3. It should be noted that only the foam is considered to have "densified" and therefore has corresponding W and C values at the point of densification. However, the stress–strain data for the polymer and the hybrid material in Table 3 are the final measured data points, i.e., $\sigma_f - e_f$, for these materials. The calculated W and C values for these materials are also for the $\sigma_f - e_f$ values. Even though the hybrid has not reached "densification" it displays the highest stress and specific energy absorbed. The foam has a cushion factor of 2.5 at densification. The cushion factor at e_f for the polymer and the hybrid are 3.9 and 3.4, respectively. The cushion factor for the hybrid material is expected to decrease and the material to demonstrate a higher energy absorption efficiency if densification is achieved by a higher impact energy.

The stress–strain curve of the hybrid specimen can also be compared to the linear addition of the stress–strain curves of the parent materials as shown in Fig. 7. Similar to the case of static testing, the stress–strain curve of the hybrid material displays a larger slope compared to the linear addition of the stress–strain curve of the parent materials prior to $e \approx 0.2$. The slope then appears to decrease to a level lower than that of the linear addition of the curves for the parent materials. As in the case of the static testing, the initial increased slope provides evidence for the interactions between the foam ligaments and the polymer filling during loading.

Due to an incomplete stress–strain curve for both the hybrid and the polymer, it is difficult to perform an in-depth comparison of energy absorption behavior between the three materials. Figure 11 shows the specific energy absorbed vs. stress for the three materials when dynamically loaded according to the current testing conditions. Ignoring the false fluctuations, the hybrid specimens show a near linear increase in the $\log(W)$ with $\log(\sigma)$. The slope is steeper than that for the polymer, but not vertical as that seen for aluminum foam. The energy absorption of the foam is approximately 10 times that of the hybrid material at the low stress levels below 3 MPa. Conversely, the hybrid specimen absorbs 15 times more energy compared to the foam as the stress increases from

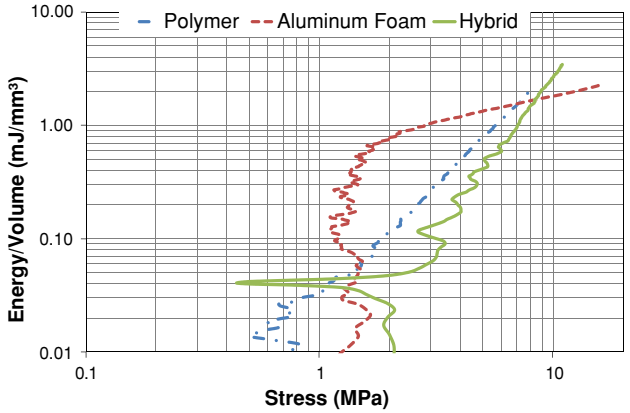

Fig. 11 Energy absorption curves for the polymer, aluminum foam, and aluminum foam–polymer hybrid under dynamic compression

3 to 10 MPa (i.e., from approximately 0.1 to 3.0 mJ/mm^3 in the hybrid and 1 to 2 mJ/mm^3 in the foam). Considering the current testing conditions, it can be concluded that aluminum foam performs better than the current prototype aluminum foam–polymer hybrid at low-stress energy absorption applications, whereas the hybrid material has a better performance at high-stress applications. Comparing the hybrid material and the polymer, the polymer has a higher energy absorption level for a comparable stress. However, the increase in the level of energy absorption with increase in stress is larger in the hybrid material for the entire stress regime achieved during current testing.

Strain rate sensitivity

As demonstrated in Fig. 8, the aluminum foam specimen does not show any measurable strain rate sensitivity for the strain rates studied in this work. This is in agreement with the previous results published by Deshpande and Fleck [7], Dannemann and Lankford Jr. [6], and McArthur et al. [12]. With little to no change in the stress–strain behavior, the energy absorption in the aluminum foam is also unchanged with strain rate.

Unlike the aluminum foam, both the polymer and the aluminum foam–polymer hybrid materials show significant strain rate dependencies. As shown in Figs. 9 and 10, in both materials, the slopes of the stress–strain curves increase with increasing the strain rate from 0.01 to 100 s^{-1}. Polymers are viscoelastic in nature and at higher loading rates, less time is allowed for stress relaxation in the viscous component, causing an increase in the apparent stiffness [36]. As the unfilled foam is not sensitive to the current change in the strain rate, the strain rate sensitivity of the hybrid material is attributed to the behavior of the polymer filling. It is therefore expected that the strain rate sensitivity of the hybrid material will change by altering the polymer filling.

The rate sensitivity also should have an impact on the energy absorption behavior. Compared to the aluminum foam which shows little change in the energy absorbed and cushion factor, the polymer and hybrid show an increasing trend in both specific energy absorption and cushion factor with the change in strain rate. However, a direct comparison of the total energy absorption efficiency in the hybrid material (or similarly in the polymer) with increasing the strain rate from 0.01 to 100 s^{-1} is not possible due to the fact that densification was not achieved with the current dynamic testing. Figure 10, however, indicates that stress–strain curve of the prototype hybrid material tested under dynamic conditions has a larger slope compared to the slope of the curve obtained under static testing conditions. This behavior, in general, can lead to a higher cushion factor and therefore a decrease in energy absorption efficiency with increasing strain rate. On the other hand, the higher stress values at high strain rates result in a higher specific energy absorbed. An important aspect of the rate sensitivity is that a hybrid material with higher energy absorption efficiency under one loading condition, compared to its parent materials, may not provide the same higher efficiency at a different loading rate. These issues highlight the importance of a comprehensive materials design/selection strategy, where variable loading conditions and the strain rate dependencies of the hybrid and its parent materials are all taken into account. It is suggested that further modeling work, as well as verifying experimental tests at multiple strain rates, be performed to provide a systematic assessment of the compressive energy absorption behavior of metal foam–polymer hybrid materials.

Summary and conclusions

The mechanical behavior or a new prototype aluminum foam–polymer hybrid material is studied under two selected static and dynamic compression testing conditions. In both loading conditions, the hybrid material demonstrates similar as well as distinct behavior when compared to the behavior of its parent materials. The observed similarities and distinctions are attributed to the level of interactions between the two hybrid components as well as the stiffness, elastic–plastic behavior, load carrying capacity, and the failure of the individual parent materials. The analysis of the energy absorption behavior at static compression loading suggests that the current prototype hybrid material has a better energy behavior at high stress levels, whereas the parent aluminum foam is a better energy absorber at low stress levels. Unlike aluminum foam, the stress–strain and energy absorption behavior of aluminum foam–polymer hybrid is found to be strain rate dependent. This is

attributed to the viscoelastic behavior of the polymer component of the hybrid.

Acknowledgements The authors would like to thank Dr. Sassan Hojabr and DuPont for their advice in the polymer selection and providing the polymer material used in this investigation. The authors would also like to extend their appreciation to Prof. Michael Worswick for the provision of the drop tower facility and Chris Salisbury and Allan Thompson for their assistance in dynamic testing. Financial support for this investigation was provided by University of Waterloo and the Natural Sciences and Engineering Research Council of Canada (NSERC).

References

1. Ashby MF, Bréchet YJM (2003) Acta Mater 51:5801
2. Kromm FX, Quenisset JM, Harry R, Lorriot T (2002) Adv Eng Mater 4:371
3. Gibson LJ, Ashby MF (1982) Proc R Soc Lond A 382:43
4. Maiti SK, Gibson LJ, Ashby MF (1984) Acta Metall 32(11):1963
5. Gibson LJ, Ashby MF (1998) Cellular solids: structure and properties, 2nd edn. Cambridge University Press, Cambridge
6. Dannemann KA, Lankford J Jr (2000) Mater Sci Eng A 293:157
7. Deshpande VS, Fleck NA (2000) Int J Impact Eng 24:277
8. Gibson LJ (2000) Annu Rev Mater Sci 30:191
9. Andrews EW, Gioux G, Onck P, Gibson LJ (2001) Int J Mech Sci 43:701
10. Banhart J (2001) Prog Mater Sci 46:559
11. Kwon YW, Cooke RE, Park C (2003) Mater Sci Eng A 343:63
12. McArthur J, Salisbury C, Cronin D, Worswick M, Williams K (2003) Shock Vibration 10:179
13. Zhou J, Gao Z, Cuitino AM, Soboyejo WO (2004) Mater Sci Eng A 386:118
14. Wang Q, Fan Z, Gui L (2006) Int J Solids Struct 43:2064
15. Zhihua W, Hongwei M, Longmao Z, Guitong Y (2006) Scr Mater 54:83
16. Bin J, Zejun W, Naiqin Z (2007) Scr Mater 56:169
17. Vamsi Krishna B, Bose S, Bandyopadhyay A (2007) Mater Sci Eng 452–453:178
18. Harte AM, Fleck NA, Ashby MF (1999) Acta Mater 47(8):2511
19. Hanssen AG, Langseth M, Hopperstad OS (2000) Int J Impact Eng 24:347
20. Tagarielli VL, Fleck NA, Deshpande VS (2004) Adv Eng Mater 6(6):440
21. Cheng HF, Han FS (2003) Scr Mater 49:583
22. Cheng HF, Huang XM, Xue GX, Li JR, Han FS (2004) Trans Nonferr Met Soc China 14(5):928
23. Jhaver R, Tippur H (2009) Mater Sci Eng A 499:507
24. Stöbener K, Lehmus D, Avalle M, Peroni L, Busse M (2008) Int J Solids Struct 45:5627
25. Wang JF, Liu XY, Luan B (2008) J Mater Process Technol 197:428
26. DuPont™ (2005) DuPont Packaging and Industrial polymers: DuPont™ Elvax® 205 W, Doc. Ref. nn3bjbm8.pdf, April 2005 Copyright 2005 E.I. du Pont de Nemours and Company, Inc
27. DuPont™ (2005) DuPont Industrial Polymers: DuPont™ Elvax®. http://www.dupont.com/industrial-polymers/elvax/H-49653-1/H-49653-1.html. Accessed 9 Sept 2005
28. Cluff DRA (2007) Fabrication of a new model hybrid material and comparative studies of its mechanical properties. MASc Thesis, University of Waterloo
29. Thompson AC (2006) High strain rate testing of advanced high strength steels. MASc Thesis, University of Waterloo
30. Hsiao HM, Daniel IM (1998) Composites Part B 29:521
31. Fuganti A, Lorenzi L, Hanssen AG, Langseth M (2000) Adv Eng Mater 2(4):200
32. Doman D (2004) Modeling of the high rate behaviour of polyurethane rubber. MASc Thesis, University of Waterloo
33. Nielson LE (1974) Mechanical properties of polymers and composites, vol 2. Marcel Dekker, New York
34. Lifshitz JM, Gov F, Gandelsman M (1995) Int J Impact Eng 16(2):201
35. Shin HS, Lee HM, Kim MS (2000) Int J Impact Eng 24:571
36. Kaelble DH (1964) In: Internal friction, damping and cyclic plasticity: a symposium presented at the sixty-seventh annual meeting. ASTM, Philadelphia